Pergamon

TETRAHEDRON

Tetrahedron 58 (2002) 2389–2395

Pyridazine derivatives. Part 27: A joint theoretical and experimental approach to the synthesis of 6-phenyl-4,5-disubstituted-3(2*H*)-pyridazinones☆

Eddy Sotelo,[a] Nuria B. Centeno,[b] Jordi Rodrigo[b] and Enrique Raviña[a,*]

[a]*Departamento de Química Orgánica, Laboratorio de Química Farmacéutica, Facultad de Farmacia, Universidad de Santiago de Compostela, Santiago de Compostela 15706, Spain*
[b]*Research Group on Biomedical Informatics, IMIM, UPF, Carrer Dr Aiguader 80, E-08003 Barcelona, Spain*

This paper is dedicated to Professor Margarita Suárez of the University of Havana, Cuba, on the occasion of her 56th birthday.

Received 12 October 2001; revised 21 January 2002; accepted 30 January 2002

Abstract—A theoretical study of the structures of a series of 5-substituted-6-phenyl-3(2*H*)-pyridazinones has been carried out using quantum-mechanical calculations. This study indicates a significant effect of the nature of the substituent at the 5-position on the reactivity of this system. The results have also been confirmed by means of ^{1}H NMR measurements. The outcome of this work has guided the development of novel and efficient synthetic pathways to obtain pharmacologically useful 6-phenyl-4,5-substituted-3(2*H*)-pyridazinones.

1. Introduction

The need to prevent thrombus formation without impairing haemostasis has spurred extensive research aimed at the development of non-thrombotic haemostatic agents and platelet aggregation inhibitors. Current therapeutic strategies to inhibit platelet function include the use of Aspirin, Triflusal (trifluoromethylaspirin), Ticlopidine, Sulfinpyrazone, or Dipyridamole. However, most of these compounds have a relatively low activity and the search for promising new drugs in this therapeutic area is of great interest. The cyclic adenosine monophosphate (c-AMP) phosphodiesterase III (PDE III) has been one of the most studied targets in the search for new antiplatelet agents.[2] Among the extensive family of PDE III inhibitors, compounds containing the 3(2*H*)-pyridazinone ring have been widely studied[3–5] and several pyridazinones, such as Zardaverine and Pimobendan (Fig. 1), have been selected for further clinical assays.[5]

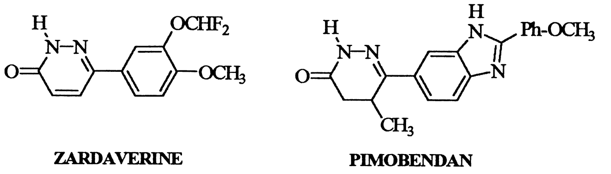

Figure 1. Chemical structure of pyridazinones Zardaverine and Pimobendan.

In the past we have studied the platelet inhibitory activity of a series of 6-aryl-3(2*H*)-pyridazinones substituted at the 5-position.[6–11] Preliminary pharmacological results reveal that these compounds, unlike other pyridazinones, have a mechanism that is not based on c-AMP PDE III but instead their activity could be related to their capacity to inhibit the influx of calcium to the activated platelets.[12]

More recently we have prepared a large number of 5-substituted-6-phenyl-3(2*H*)-pyridazinones and tested their antiplatelet activity.[13,14] The structure–activity relationship studies (SAR) on this series has shown that the most active compounds are those that bear electron-withdrawing groups in the 5-position (e.g. CHO, COOMe, CH_2OCOCH_3); conversely, compounds containing electron-releasing groups (e.g. NH_2, $NHNH_2$) are completely inactive.[14] In light of these results, we have concluded that the antiplatelet activity in this series is determined by the chemical group present at the 5-position of the 6-phenyl-3(2*H*)-pyridazinone system.[14]

Taking into account these conclusions, and in order to achieve a better understanding of the chemical basis for the antiplatelet activity, we decided to carry out a quantum-chemical characterisation of a subset of several representative 5-substituted-6-phenyl-3(2*H*)-pyridazinones. In the work described in this paper we evaluated the influence of the nature of the substituent at the 5-position on the

---

☆ See Ref. 1.

Keywords: pyridazinones; conformational analysis; ESP charges.

* Corresponding author. Fax: +34-981-594912; e-mail: qofara@usc.es

0040–4020/02/$ - see front matter © 2002 Elsevier Science Ltd. All rights reserved.
PII: S0040-4020(02)00120-5

reactivity of the heterocyclic ring. In addition, we explored the synthetic possibilities arising from the use of the appropriate 5-substituted-6-phenyl-3(2*H*)-pyridazinones as starting materials in the preparation of 6-phenyl-4,5-substituted-3(2*H*)-pyridazinones.

These results have particular preparative importance since very few methods based on the direct introduction of a substituent at the 4-position of 5-substituted-3(2*H*)-pyridazinones have been described.[15] Indeed, the methods that have been reported usually use as starting materials *N*-protected pyridazinones that have protecting groups that are either very difficult or impossible to remove. Therefore, methods for the direct introduction of substituents into the pyridazinone ring are lacking and new developments are of great interest because they should provide access to a wide variety of pharmacologically useful 4,5-disubstituted compounds.

2. Results and discussion

The synthesis of the 3(2*H*)-pyridazinones **1a**–**f** (Table 1) has previously been described by our group.[11,13] These compounds have not been subjected to a detailed structural examination until now and we report here the first computational study on the structure–reactivity relationship in this series.

To this end, we initially determined the favoured geometry of the compounds in question (**1a**–**f**) by means of a systematic conformational search at the ab initio Hartree–Fock level using the 3-21G basis set (3-21G* for compound **1d**). Preliminary semiempirical molecular orbital calculations (data not shown), both in the gas phase and in solution, failed to reproduce the results obtained from IR and ^{13}C NMR experiments (Table 1), suggesting that the keto form is the predominant one. Conversely, ab initio HF/3-21G results indicate that the keto form is more stable than the enol form by about 10 kcal/mol (Table 2). We therefore decided to carry out our conformational search at the HF/3-21G level despite its greater computational cost. The results of the energy calculations on the keto–enol tautomerism show that the presence of electron-releasing groups at the 5-position stabilise the keto form to a greater extent, as can be seen from the data in Table 2.

Table 1. Structure and representative spectroscopic data of the 6-phenyl-5-substituted-3(2*H*)-pyridazinones studied

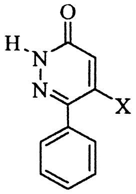

Compound	X	Absorption band of the C=O (cm^{-1})	Chemical shift for C=O (ppm)	Chemical shift for H_4 (ppm)
1a	H	1644	160	6.98
1b	CHO	1650	159	7.37
1c	CN	1672	163	7.84
1d	SO_2CH_3	1695	159	7.88
1e	NH_2	1670	162	5.73
1f	OCH_2CH_3	1656	162	6.36

Table 2. Energetic differences between the keto and enol forms

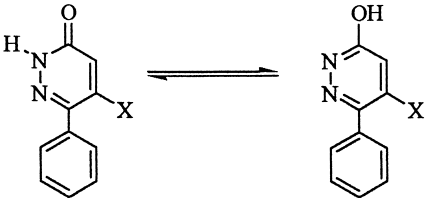

Compound	X	ΔEnergy (keto–enol) in kcal/mol
1a	H	9.77
1b	CHO	9.12
1c	CN	9.49
1d	SO_2CH_3	9.44
1e	NH_2	10.31
1f	OCH_2CH_3	10.89

The lowest energy conformation of the keto form obtained from HF/3-21G ab initio calculation (HF/3-21G* for compound **1d**), was the starting point for the enol tautomer geometry, which was fully optimised at the same quantum-mecanical level. Then, energies of the enol and keto forms were compared to establish which is more stable.

The geometrical features of the lowest energy conformation found for each compound are shown in Fig. 2. The conformational analysis of this series shows that the phenyl substituent in position 6 is not coplanar with the pyridazinone ring. The degree of deviation ranges from 24 to 53° (Table 3) depending on the nature of the substituent. Rather than the total volume of the substituent at position 5, the degree of deviation seems to be related to the steric hindrance caused by the moiety directly attached to the carbon atom at position 5. The relatively low deviation observed in **1f** is probably due to the fact that the ethyl moiety is in its all-extended conformation, whereas the compound with the most marked deviation (**1d**) has not only a voluminous group (SO_2) attached to C5 but also a methyl group in the $g+$ conformation.

The results of the theoretical calculations were compared, wherever possible, with the data obtained by X-ray crystallography. We found a different degree of agreement between the conformations characterised quantum-mechanically and those determined by X-ray analysis (Table 3). The lowest energy conformation found for compound **1e** matches its X-ray structure.[16] The X-ray structure of compound **1f** (Fig. 3), however, contains three molecules in the asymmetric unit, one of which is very similar to the lowest energy conformation found in our calculations. The greatest discrepancies arise in the case of compound **1d**, where we believe that the conformation exhibited in the X-ray structure (Fig. 3) is probably influenced by the packing forces in the crystal. Overall, these findings all suggest that the energy barrier of the torsional angle between the pyridazinone and the phenyl ring should be very low and is influenced by both the substituent in position 5 and the environment.

Taking into account the important modifications caused by the chemical group at position 5 on the H_4 signal in the ^1H

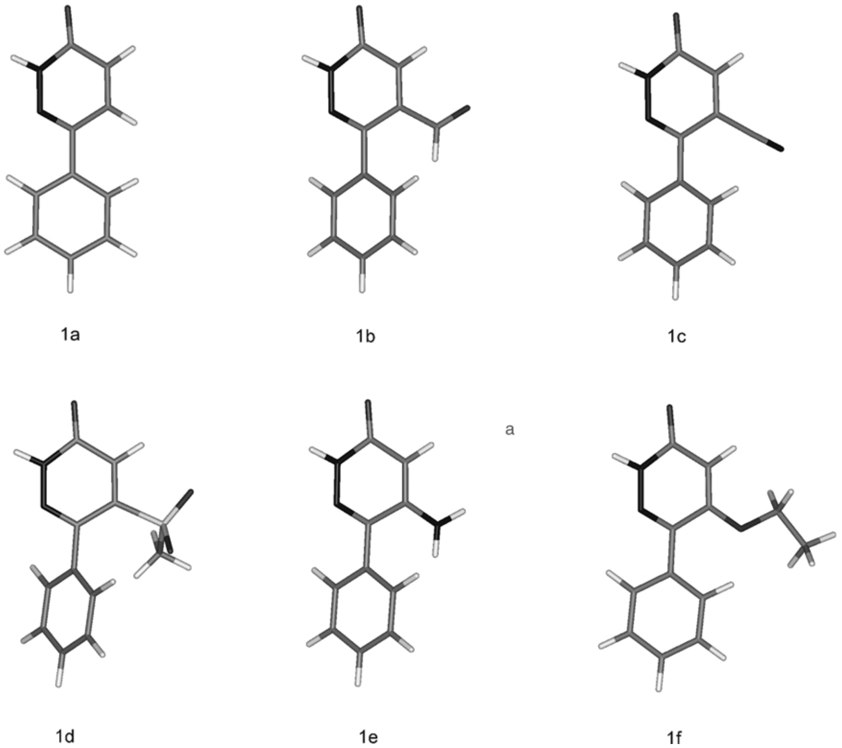
1a 1b 1c

1d 1e 1f

Figure 2. Ab initio HF/3-21G (HF/3-21G* for compound **1d**) optimised geometries for the lowest energy conformations of compounds **1a**–**1f**.

Table 3. Characterisation of lowest energy conformations of the six compounds studied quantum-mechanically and comparison with X-ray data (where available)

Compound	X	Calculated conformation		X-Ray conformation	
		N1–C6–C1′–C2′ (in °)[1]	Conformation of the 5-substituent (°)	N1–C6–C1′–C2′ (°)	Conformation of the 5-substituent (°)
1a[2]	H	24.4	–		–
1b[2]	CHO	51.2	−174.6		
1c[2]	CN	44.2	–		–
1d	SO_2CH_3	53.1	60.6	92.0	81.9
1e	NH_2	52.3	–	−51.3	–
1f	OCH_2CH_3	31.4	174.3; −176.5	32.7	−173.3; 163.4

[a] For each compound, another conformation with the same value of the dihedral N1–C6–C1′–C2′, but opposite sign is found that is energetically degenerate.

[b] X-Ray data are not available.

NMR spectra (Table 1) of compounds in this series, we can hypothesize about the synthetic exploitation of these systems. In order to analyse the electronic characteristics of the 4-position, we calculated the partial charge at this site. In order to obtain accurate values we calculated the ESP fitting charges using the Merz–Kollman atomic radii at the HF/6-21G level (HF/6-21G* for compound **1d**). The predicted values are shown in Table 4 and are in reasonably good agreement with the experimental data (^1H NMR). Interestingly, the results highlight the importance of the electronic characteristics of the carbon atom in the 4-position, a feature that has been confirmed by ^1H NMR data on the series of compounds under investigation. Analysis of the partial charge values shows, as one would expect, a notable change in the electronic nature of C_4 due to the electronic effect of the chemical group at position 5. The presence of electron-withdrawing groups in the 5-position produces a significant decrease in the negative charge at the

Table 4. Calculated partial charges at the 4-position

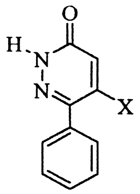

Compound	X	Partial charge at the 4-position
1e	NH_2	−0.4927
1f	OCH_2CH_3	−0.3773
1a	H	−0.1255
1c	CN	−0.0532
1b	CHO	−0.0327
1d	SO_2CH_3	−0.0274

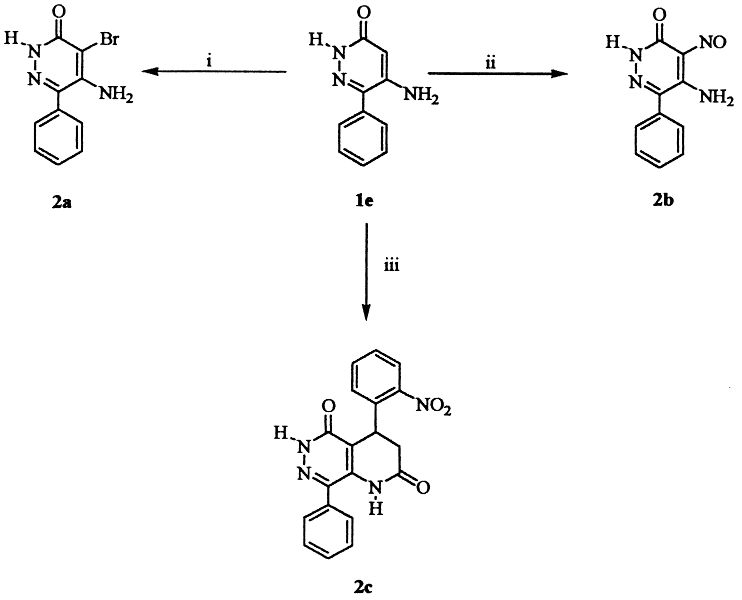

Scheme 1. *Reagents*: (i) Br_2/AcOH, (ii) $NaNO_2$/AcOH, (iii) 5-(2-Nitroarylidene)-2,2-dimethyl-1,3-dioxan-4,6-dione/MeOH.

4-position (by a factor of 4 in **1d** with regard to **1a**), thus generating an electrophilic character at position 4. On the other hand, the presence of electron-releasing groups in the 5-position generates nucleophilic character at C_4. The strategical placement of the substituent at the end of the double bond of the d face of the heterocyclic ring and the presence of a carbonyl group both have important repercussions on the reactivity of the 4-position of the diazinone system.

By considering all these predictions, and also on the basis of the modifications in the reactivity at the 4-position caused by the electronic effect of the neighbouring group, we have developed novel and highly efficient synthetic alternatives that allow the synthesis of 4,5-substituted-3(2*H*)-pyridazinones and heterobicyclic compounds.

Firstly, we studied the reactivity of the heterocyclic enaminone **1e**, the strong push–pull effect on this compound facilitates their reaction with different electrophiles (Scheme 1). Compound **1e** (in accordance with its enamine nature) can be easily brominated in the 4-position by treatment with bromine in acetic acid to afford compound **2a**. In turn, nitrosation of **1e** gives the 5-amino-4-nitroso-6-phenyl-3(2*H*)-pyridazinone **2b** as a deep-red solid in excellent yield. Compound **1e** also shows high reactivity towards Michael addition and, therefore, reaction of **1e** with 5-arylidene Meldrum's acid derivatives as Michael donors—following a Hantzsch-like approach—involving the imino–enamine tautomerism and subsequent 6-*exo-trig* cyclization that allows the annulation of the heterocycle. This process leads to the bicyclic 2,5-dioxo-4-(2-nitrophenyl)-8-phenyl-1,2,3,4,5,6-hexahydropyrido[2,3-*d*]-pyridazine **2c** in high yield, as we described recently.[17]

In contrast, compounds **1b** and **1g**, which have electron-withdrawing groups at position 5, show a high reactivity towards the cyanide anion. Thus, treatment of **1b** or **1g** with an excess of sodium cyanide in methanol gives compounds **2d** and **2e** in high yield (Scheme 2). These products have a cyano group in the 4-position. The synthesis of **2d** and **2e** represents the first direct cyanation on a pyridazinone ring.[18] The proposed mechanism for this transformation involves the 1,4-addition of cyanide to the α,β-unsaturated system and subsequent spontaneous aromatization of the 4,5-dihydro-3(2*H*)-pyridazinone intermediate, which was not isolated. Finally, 1,2-addition of cyanide to the formyl group in **1e** leads to the cyanhydrine **2d**. This mild and efficient multi-step one-pot reaction is the subject of further study in our laboratory in order to assess the limits of this approach.

The 3(2*H*)-pyridazinones **2a–2e** that were prepared were fully characterised by their analytical and spectroscopic data. The IR spectra of compounds **2a–2e** contain peaks showing presence of NH and carbonyl groups at 3380–3280 and 1680 cm^{-1}, respectively. The structures of these compounds can be easily confirmed by the absence of the H_4 signal in the ^1H NMR spectra. Further experiments are now in progress aimed at obtaining new 4,5-substituted

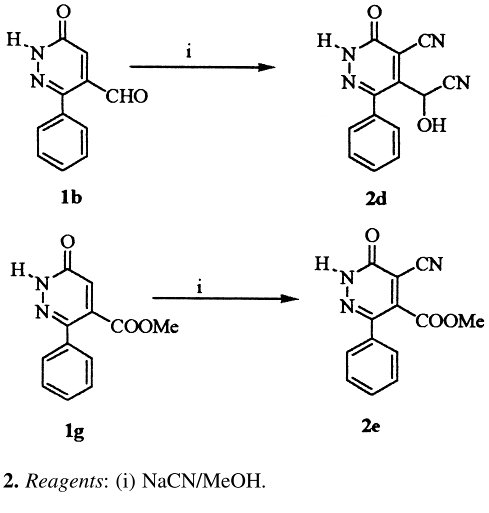

Scheme 2. *Reagents*: (i) NaCN/MeOH.

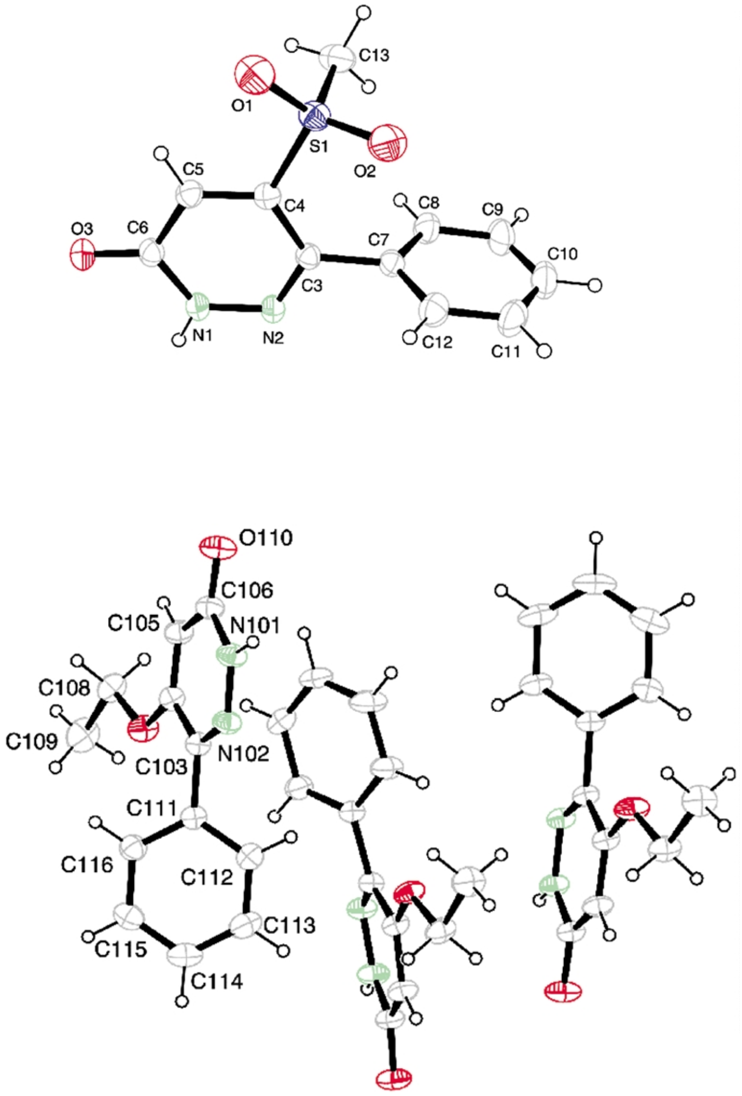

Figure 3. X-Ray structure of compounds **1d** and **1f**.

pyridazinones and evaluating the effect of the new group on the antiplatelet activity of compounds in this series.

In summary, we have described a structural study that has allowed the evaluation of the effect of the substituent at position 5 on the reactivity of compounds in this series. These results have been used to support the development of novel and efficient synthetic procedures to prepare highly functionalized and heterofused pyridazinones using 5-substituted-6-phenyl-3(2*H*)-pyridazinones as starting materials. In light of these results, and taking in account our previous pharmacological results, we can clearly conclude that the nature of the group in the 5-position of the 6-phenyl-3(2*H*)-pyridazinone system not only determines the pharmacological activity but also produces a notable, and synthetically exploitable, modification in the reactivity of the heterocyclic ring.

3. Experimental

Melting points were determined on a Gallenkamp melting point apparatus and are uncorrected. IR spectra were measured using a Perkin–Elmer 1640 FTIR spectrophotometer with samples as potassium bromide pellets. The NMR spectra were recorded on Bruker AM300 and XM500 spectrometers. Chemical shifts are given as δ values against tetramethylsilane as internal standard and J values are given in Hz. Mass spectra were determined on a Varian MAT-711 instrument. High resolution mass spectra of compound **2d** was determined on a Autospec Micromass. Elemental analyses were performed on a Perkin–Elmer 240B apparatus at the Microanalysis Service of the University of Santiago de Compostela. The reactions were monitored by TLC with 2.5 mm Merck silica gel GF 254 strips, and the purified compounds each showed a single spot; unless stated otherwise, iodine vapour and/or UV light were used for detection of compounds. Commercially available starting materials and reagents were purchased from commercial sources and were used without further purification.

3.1. Computational details

Three-dimensional models of the studied compounds were initially built using the Builder module of InsightII (v. 95.0, from Biosym/MSI, San Diego, CA, USA). A systematic search using an increment of 30° for every considered dihedral angle was carried out. Those conformations exhibiting bumps were discarded as starting points. The geometries of the selected starting points were fully optimised quantum-mechanically by energy minimisation at the ab initio Hartree–Fock level, using the 3-21G basis set (or 3-21G* in the case of compound **1d** because of the presence of a sulfur atom). Starting from the lowest energy conformation obtained, a point calculation at HF/6-31G level (HF/6-31G* for compound **1d**) was used to fit ESP charges using the Merz–Kollman radii. The GAUSSIAN 94 program (Gaussian Inc., Pittsburgh, PA, USA) was used throughout all quantum-mechanics computations.

3.2. X-Ray structure analysis

Crystals of **1d** and **1f** (Fig. 3) were grown by slow evaporation from ethanol solutions. The X-ray determination was performed on a MACH3 Enraf Nonius diffractometer with graphite monochromated Cu Kα radiation.

3.2.1. 5-Methylsulfonyl-6-phenyl-3(2*H*)-pyridazinone (1d). *Crystal data*. $C_{11}H_{10}N_2O_3S$, $M=250.27$, orthorhombic, $a=7.4065$ (6), $b=10.4442$ (8), $c=28.7383$ (17) Å, $\beta=90.00°$, $V=2223.1$ (3) Å^3 by least-squares refinement on diffractometer angles for 25 automatically centred reflections with $18.91<\theta<42.89°$, $\lambda=1.54184$ Å, $T=293(2)$ K, space group *Pbca*, $Z=8$, $D_c=1.496$ Mg/m^3, $\mu=2.599$ mm^{-1}. A colourless prismatic crystal (0.32×0.24×0.08 mm^3) was used for the analysis. Detailed crystallographic data for compound **1d** have been deposited at the Cambridge Crystallographic Data Centre (deposition number CCDC 166861) and are available on request.

3.2.2. 5-Amino-6-phenyl-3(2*H*)-pyridazinone (1e). *Crystal data*. $C_{10}H_9N_3O$, $M=187.20$, Orthorhombic, *Pbca*, $a=8.752$ (2), $b=10.525$ (5), $c=20.619$ (5) Å, $V=1899.3$ (11) Å^3 by least-squares refinement on diffractometer angles for 25 automatically centred reflections with $10.78<\theta<28.12°$, $\lambda=1.54184$ Å, $T=293(2)$ K, space group *Pbca*, $Z=8$, $D_c=1.309$ Mg/m^3, $\mu=0.73$ mm^{-1}. A light-green prismatic crystal (0.48×0.20×0.14 mm^3) was used for the analysis. Detailed crystallographic data for compound **1e** have been deposited at the IUCr electronic archives (deposition number SK1336) and are available on request.

3.2.3. 5-Ethoxy-6-phenyl-3(2*H*)-pyridazinone (1f). *Crystal data*. $C_{12}H_{12}N_2O_2$, $M=216.24$, monoclinic, $a=13.0709(13)$, $b=7.6595(7)$, $c=16.4920(13)$ Å, $\beta=99.130(8)°$, $V=1643.4(3)$ Å^3 by least-squares refinement on diffractometer angles for 25 automatically centred reflections with 21.65–42.69°, $\lambda=1.54184$ Å, $T=293(2)$ K, space group $P2_1$, $D_c=1.321$ Mg/m^3, $\mu=0.751$ mm^{-1}. A colourless prismatic crystal (0.44×0.32×0.20 mm^3) was used for the analysis. Detailed crystallographic data for compound **1f** have been deposited at the Cambridge Crystallographic Data Centre (deposition number CCDC 166799) and are available on request.

3.2.4. 5-Amino-4-bromo-6-phenyl-3(2*H*)-pyridazinone (2a). To a mixture of 5-amino-6-phenyl-3(2*H*)-pyridazinone (**1e**) (0.70 g, 3.7 mmol) and sodium acetate trihydrate (0.66 g, 4.8 mmol) in acetic acid (15 mL) at 0°C was added slowly a solution of bromine (0.65 mL, 4.4 mmol) in acetic acid (3 mL). The resulting mixture was stirred at room temperature during 45 min and then added to ice/water. The solid that precipitated was collected by filtration. Further purification was carried out by recrystallization from isopropanol to give 0.91 g of **2a** as a white solid (92%). Mp 323.4–325.0°C (dec.), IR: ν_{max}/cm^{-1} 3422–3185 (NH_2), 1643 (CO), 1578 (aromatics); ^{1}H NMR: δ_H (300 MHz, DMSO-d$_6$) 12.64 (1H, brs, NH, deuterium oxide exchangeable), 7.48 (5H, m, aromatics), 6.04 (2H, brs, deuterium oxide exchangeable, NH_2). $C_{10}H_8BrN_3O$ requires C: 45.13; H: 3.03; N: 15.79, found: C: 45.21; H: 3.17; N: 15.72.

3.2.5. 5-Amino-4-nitroso-6-phenyl-3(2*H*)-pyridazinone (2b). To a solution of 5-amino-6-phenyl-3(2*H*)-pyridazinone (**1e**) (0.50 g, 2.7 mmol) in a 1:1 mixture of acetic acid/water (25 mL) at 65°C was added slowly a solution of sodium nitrite (0.36 g, 5.3 mmol) in water (4 mL). The reaction mixture was stirred at 65°C during 2 h and the solid that precipitated was collected by filtration. Further purification was carried out by recrystallization from a 1:1 mixture of ethyl acetate/methanol to give 0.45 g of **2b** as a red solid (80%). Mp 238.7–240.0°C (dec.), IR: ν_{max}/cm^{-1} 3422–3185 (NH_2), 1633 (CO), 1588 (aromatics); ^{1}H NMR: δ_H (300 MHz, DMSO-d$_6$) 12.39 (1H, brs, NH, deuterium oxide exchangeable), 7.90 (2H, m, aromatics), 7.40 (3H, m, Aromatics), 3.38 (2H, brs, deuterium oxide exchangeable, NH_2). HRMS *m/z* calcd for $C_{10}H_8N_4O_2$ (M^+): 216.1963, found: 216.1952.

3.2.6. 2,5-Dioxo-4-(2-nitrophenyl)-8-phenyl-1,2,3,4,5,6-hexahydropyrido[2,3-*d*]pyridazine (2c). An equimolecular mixture of 5-(2-nitroarylidene)-2,2-dimethyl-1,3-dioxan-4,6-dione (40 mmol) and 5-amino-6-phenyl-3(2*H*)-pyridazinone (**1e**) in methanol (50 mL) was refluxed during 20 h and the resulting solution was poured into ice/water. The solid that precipitated was collected by filtration and recrystallized from ethanol to give **2c** as a white solid (90%). Mp 264.0°C (dec.), IR: ν_{max}/cm^{-1} 3384 (NH), 3111 (CH), 1715, 1645 (C=O), 1576, 1518 (C=C), 1530 (NO_2) and 1341 (NO_2); ^{1}H NMR: δ_H (300 MHz, DMSO-d$_6$) 13.09 (1H, brs, NH, deuterium oxide exchangeable), 9.53 (1H, brs, NH, deuterium oxide exchangeable), 8.01 (1H, dd, $J=7.7$, 0.9 Hz, aromatics), 7.61–7.49 (2H, m, Ph), 7.47 (5H, s, aromatics), 7.18 (1H, dd, $J=7.7$, 0.9 Hz, aromatics), 4.78 (1H, dd, $J=7.2$, 1.6 Hz, H-4), 3.34 (1H, dd, $J=7.2$, 9.6 Hz, H-3), 2.60 (1H, dd, $J=9.6$, 1.6 Hz, H-3′). $C_{19}H_{14}N_4O_4$ requires C: 62.98; H: 3.89; N: 15.46, found: C: 62.80; H: 3.77; N: 15.35.

3.2.7. 4-Cyano-5-(1′-cyanohydroxymethyl)-6-phenyl-3(2*H*)-pyridazinone (2d). To a stirred solution of the aldehyde **1b** (0.10 g, 0.5 mmol) in ethanol (10 mL) was added, in several portions, sodium cyanide (0.07 g, 0.15 mmol) and the stirring was maintained during 1 h. The reaction mixture was poured into ice and then extracted with ethyl acetate. The organic extracts were dried (anhydrous sodium sulfate) and concentrated under reduced pressure to give an oily residue that was purified by column chromatography (hexane/ethyl acetate, 1:1). Subsequent recrystallization from isopropanol afforded the cyanhydrine **2d** as yellow prisms (90%). Mp 145.5–147.0°C (dec.), IR (KBr): ν_{max}/cm^{-1} 3808–3065, 1663, 1590. ^{1}H NMR: δ_H (300 MHz, DMSO-d$_6$): 13.94 (1H, brs, NH, deuterium oxide exchangeable), 7.55–7.48 (5H, m, aromatics), 4.02 (1H, s, CH). HRMS (Autospec Micromass) *m*/*z* calcd for $C_{13}H_8N_4O_2$ (M^+): 252.0647, found: 252.0650.

3.2.8. 4-Cyano-5-methoxycarbonyl-6-phenyl-3(2*H*)-pyridazinone (2e). To a stirred solution of the ester **1g** (0.10 g, 0.4 mmol) in methanol (20 mL) was added slowly sodium cyanide (0.04 g, 0.8 mmol) and the stirring was maintained during 36 h at room temperature. The solvent was removed under reduced pressure and the resulting residue was poured into ice to afford a yellow solid that was purified by recrystallization from isopropanol (70%). Mp 190.2–191.0°C, IR (KBr): ν_{max}/cm^{-1} 1735, 1668, 1588. ^{1}H NMR: δ_H (300 MHz, DMSO-d$_6$): 14.63 (1H, brs, NH, deuterium oxide exchangeable), 7.50 (3H, m, aromatics), 7.40 (2H, m, aromatics), 7.36 (1H, s, OCH_3). $C_{13}H_9N_3O_3$ requires C: 61.17; H: 3.55; N: 16.46, found: C: 61.24; H: 3.55; N: 16.56.

Acknowledgements

The authors wish to express their gratitude to Dr Manuel Pastor for helpful discussions. This work was supported by the Spanish Interministerial Commission for Science and Technology (CICYT) and by the Xunta de Galicia (Project XUGA 8151389). We thank the CESCA (Centre de Supercomputació de Catalunya) for the use of computational facilities. We also thank the Spanish Instituto de Cooperación Iberoamericana (ICI) for a doctoral fellowship for Eddy Sotelo.

References

1. Part of this work was presented at the Seventh International Symposium on the Chemistry and Pharmacology of Pyridazines, Santiago de Compostela, Spain, September 13–16, 2000. For the previous paper in this series, see: Sotelo, E.; Raviña, E. Efficient and Regioselective Pd-catalysed Arylation of 4-Bromo-6-chloro-8-phenylpyridazine. *Synlett* **2002**, 223.
2. Campbell, S. F.; Danilewicz, J. C. *Ann. Rep. Med. Chem.* **1978**, *22*, 84.
3. Bristol, J. A.; Sircar, I.; Moss, W. H.; Evans, D. B.; Weishaan, E. *J. Med. Chem.* **1984**, *27*, 1099.
4. Sircar, I.; Duell, B. L.; Cain, M. H.; Burke, S. E.; Bristol, J. A. *J. Med. Chem.* **1986**, *29*, 2142.
5. Combs, D. H. *Drugs Future* **1993**, *18*, 139.
6. Raviña, E.; García-Mera, G.; Santana, L.; Orallo, F.; Calleja, J. M. *Eur. J. Med. Chem.* **1985**, *20*, 475.
7. Terán, C.; Raviña, E.; Santana, L.; García, G.; García-Mera, G.; Fontenla, J. A.; Orallo, F.; Calleja, J. M. *Arch. Pharm. (Weinheim)* **1989**, *322*, 331.
8. Raviña, E.; Terán, C.; Santana, L.; García, N.; Estévez, I. *Heterocycles* **1990**, *31*, 1967.
9. Raviña, E.; Terán, C.; Domínguez, N. G.; Masaguer, C. F.; Gil-Longo, J.; Orallo, F.; Calleja, J. M. *Arch. Pharm. (Weinheim)* **1991**, *324*, 455.
10. Estévez, I.; Raviña, E.; Sotelo, E. *J. Heterocycl. Chem.* **1998**, *35*, 1421.
11. Sotelo, E.; Raviña, E.; Estévez, I. *J. Heterocycl. Chem.* **1999**, *36*, 985.
12. Montero-Lastres, A.; Fraiz, N.; Cano, E.; Laguna, R.; Estévez, I.; Raviña, E. *Biol. Pharm. Bull.* **1999**, *22*, 1376.
13. Laguna, R.; Rodriguez-Liñares, B.; Cano, E.; Estévez, I.; Raviña, E.; Sotelo, E. *Chem. Pharm. Bull.* **1997**, *45*, 1151.
14. Sotelo, E. PhD Thesis, University of Santiago de Compostela, Spain, 2000.
15. Matyus, P.; Fuji, K.; Tanaka, K. *Heterocyles* **1994**, *37*, 171.
16. Novoa de Armas, H.; Blaton, N. M.; Peeters, O. M.; De Ranter, C. J.; Pita, B.; Sotelo, E.; Raviña, E.; Suárez, M. *Acta Crystallogr., C* **2000**, *56*, 345.
17. Pita, B.; Sotelo, E.; Suárez, M.; Raviña, E.; Ochoa, E.; Verdecia, Y.; Novoa, H.; Blaton, N.; De Ranter, C.; Peeters, O. *Tetrahedron* **2000**, *56*, 2473.
18. Sotelo, E.; Pita, B.; Raviña, E. *Tetrahedron Lett.* **2000**, *41*, 2863.